

Supplemental Information for:

**ALK and RET inhibitors promote human leukocyte antigen class
I antigen presentation and unmask new antigens within the
tumor immunopeptidome**

Claire Y. Oh^{1,2}, Martin G. Klatt¹, Elliott J. Brea^{1,2}, Tao Dao¹, Aaron
Y. Chang^{1,2}, and David A. Scheinberg^{1,2,3}

¹Molecular Pharmacology Program, Memorial Sloan Kettering
Cancer Center, New York, NY, USA 10065

²Weill Cornell Medicine, New York, NY, USA 10021

³ To whom correspondence should be addressed:
scheinbd@mskcc.org

Table of Contents for Supplementary Material

Additional Material and Methods

Supplemental Figure S1: Increase in cell surface HLA depend on decrease in pERK in ALK inhibited ALCL cells.

Supplemental Figure S2: RET inhibition leads to increase HLA.

Supplemental Figure S3: Increase in antigen processing machinery transcript and protein in ALK inhibited ALCL cells.

Supplemental Figure S4: JAK/STAT pathway in HLA regulation

Supplemental Figure S5: Cytokine secretion in response to inhibitors

Supplemental Figure S6: ALK inhibition in vivo and PD-L1 levels in vitro.

Supplemental Figure S7: Checkpoint ligands levels in response to ALK and RET inhibition.

Supplemental Figure S8: Analysis of peptide repertoire changes after RET inhibition.

Supplemental Figure S9: PBMC viability is not affected by inhibitors.

Supplemental Figure S10: HLA-E levels do not change with drug treatment.

Supplemental Table 1: Summary of the inhibitors effects on HLA, antigen processing machinery, and checkpoint ligands

Additional Material and Methods

Immunopurification of HLA class I ligands

For immunopurification affinity columns were prepared as described previously. In brief, 40 mg of Cyanogen bromide-activated-Sepharose[®] 4B (Sigma-Aldrich, Cat# C9142) was activated with 1mM hydrochloric acid (Sigma-Aldrich, Cat# 320331) for 30 min. Subsequently, 0.5 mg of W6/32 antibody (BioXCell, BE0079; RRID: [AB_1107730](#)) was coupled to sepharose in presence of binding buffer (150mM sodium chloride, 50 mM sodium bicarbonate, pH 8.3; sodium chloride: Sigma-Aldrich, Cat# S9888, sodium bicarbonate: Sigma-Aldrich, Cat#S6014) for at least 2 hours at room temperature. Sepharose was blocked for 1 h with glycine (Sigma-Aldrich, Cat# 410225). Columns were equilibrated with PBS for 10 min.

TPC1 cells were treated with DMSO, 10nM AST487, or 100nM cabozantinib. Karpas 299 cells were treated with DMSO, 100nM crizotinib or 100nM ceritinib for 72h. 20 – 30 x 10⁶ cells were harvested and washed three times in ice-cold sterile PBS (Media preparation facility MSKCC). Afterwards, cells were lysed in 1 ml 1% CHAPS (Sigma-Aldrich, Cat# C3023) in PBS, supplemented with protease inhibitors (cOmplete, Cat# 11836145001) for 1 hour at 4°C. Lysate was spun down for 1 hour with 20,000 g at 4°C. Supernatant was run over column through peristaltic pumps with 1 ml/min overnight in cold room. Affinity columns were washed with PBS for 15 min, run dry, and HLA complexes subsequently eluted three times with 200 µl 1% trifluoroacetic acid (TFA, Sigma/Aldrich, Cat# 02031). For separation of HLA ligands from their HLA complexes tC18 columns (Sep-Pak tC18 1 cc Vac Cartridge, 100 mg Sorbent per Cartridge, 37-55 µm Particle Size, Waters, Cat# WAT036820) were prewashed with 80% acetonitrile (ACN, Sigma-Aldrich, Cat# 34998) in 0.1% TFA and equilibrated with two washes of 0.1% TFA. Samples were loaded, washed again with 0.1% TFA and eluted in 400 µl 30% ACN in 0.1%TFA. Sample volume was reduced by vacuum centrifugation for mass spectrometry analysis.

LC-MS/MS analysis of HLA ligands

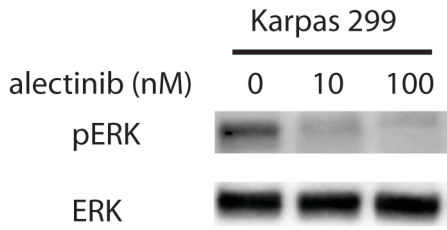
Samples were analyzed by high resolution/high accuracy LC-MS/MS (Lumos Fusion, Thermo Fisher). Peptides were desalted and concentrated prior to being separated using direct loading onto a packed-in-emitter C18 column (75µm ID/12cm, 3 µm particles, Nikkyo Technos Co., Ltd. Japan). The gradient was delivered at 300nl/min increasing linear from 2% Buffer B (0.1% formic acid in 80% acetonitrile) / 98% Buffer A (0.1% formic acid) to 30% Buffer B / 70% Buffer A, over 70 minutes. MS and MS/MS were operated at resolutions of 60,000 and 30,000, respectively. Only charge states 1, 2 and 3 were allowed. 1.6 Th was chosen as isolation window and collision energy was set at 30%. For MS/MS, maximum injection time was 100ms with an AGC of 50,000.

Mass spectrometry data processing

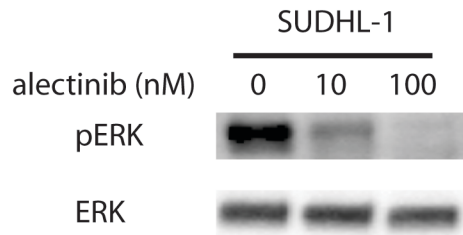
Mass spectrometry data was processed using Byonic software (version 2.7.84, Protein Metrics, Palo Alto, CA) through a custom-built computer server equipped with 4 Intel Xeon E5-4620 8-core CPUs operating at 2.2 GHz, and 512 GB physical memory (Exxact Corporation, Fremont, CA). Mass accuracy for MS1 was set to 10 ppm and to 20 ppm for MS2, respectively. Digestion specificity was defined as unspecific and only precursors with charges 1,2, and 3 and up to 2 kDa were allowed. Protein FDR was disabled to allow complete assessment of potential peptide identifications. Oxidization of methionine, N-terminal acetylation, phosphorylation of serine, threonine and tyrosine were set as variable modifications for all samples. All samples were searched against UniProt Human Reviewed Database (20,349 entries, <http://www.uniprot.org>, downloaded June 2017). Peptides were selected with a minimal log prob value of 2 resulting in a 1% false discovery rate and were HLA assigned by netMHC 4.0 with a 5% rank cutoff.

Supplemental Figure S1

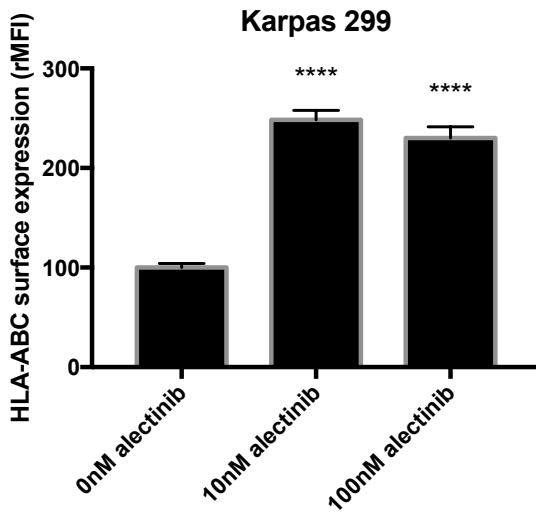
A



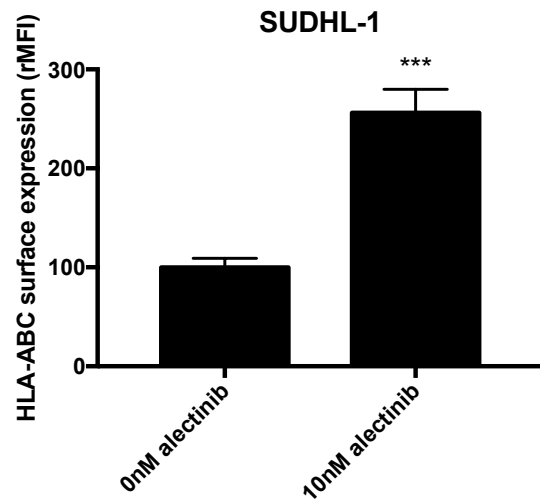
B



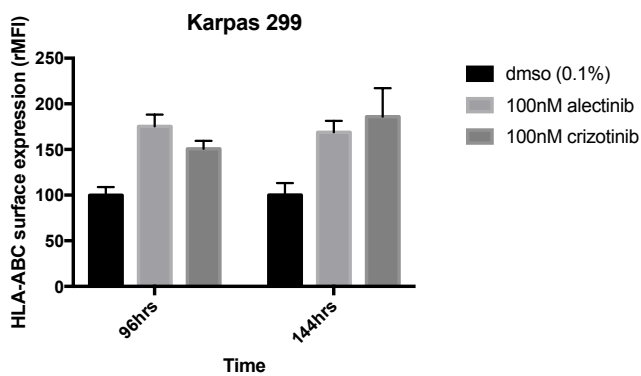
C



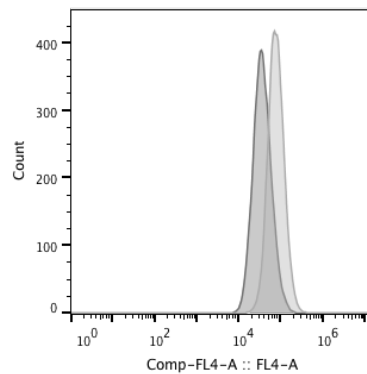
D



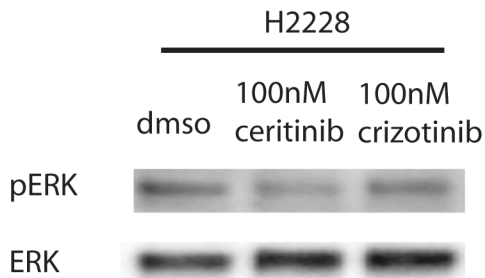
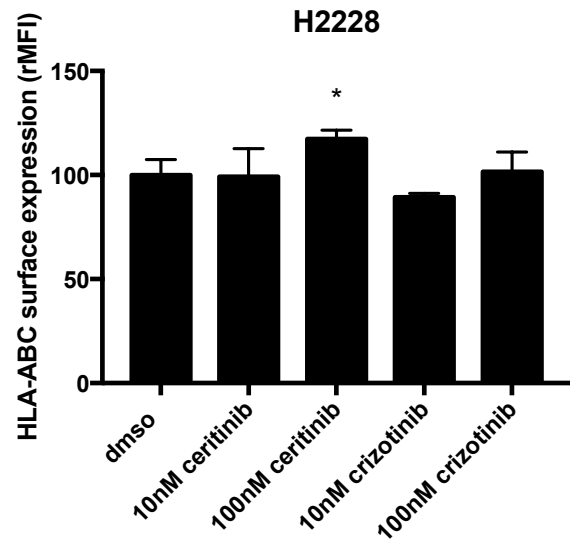
E



F



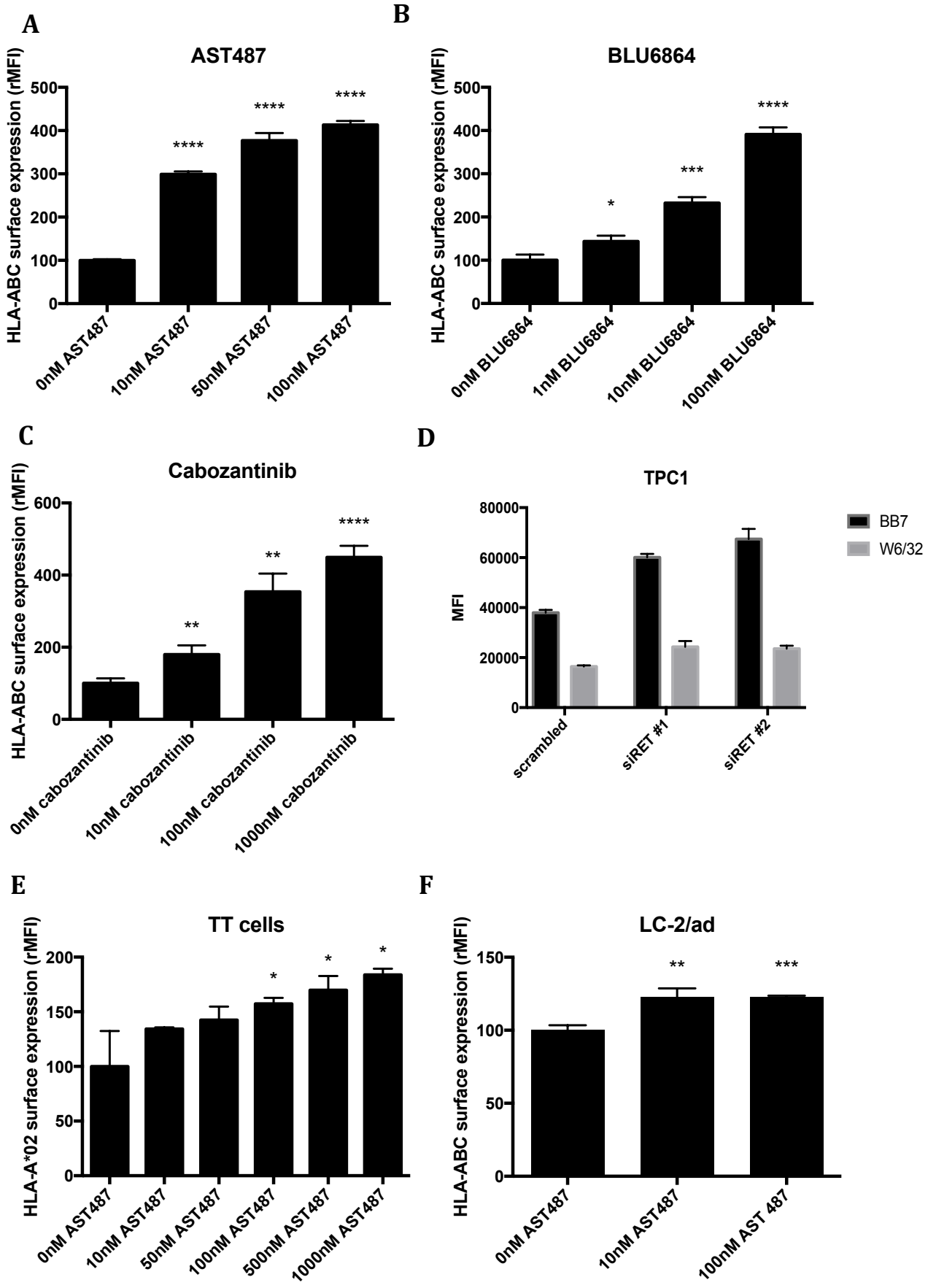
Sample Name	Subset Name
C01 Karpas_W632_100nM criz.fcs	PI negative
B01 Karpas_W632_dms0.fcs	PI negative

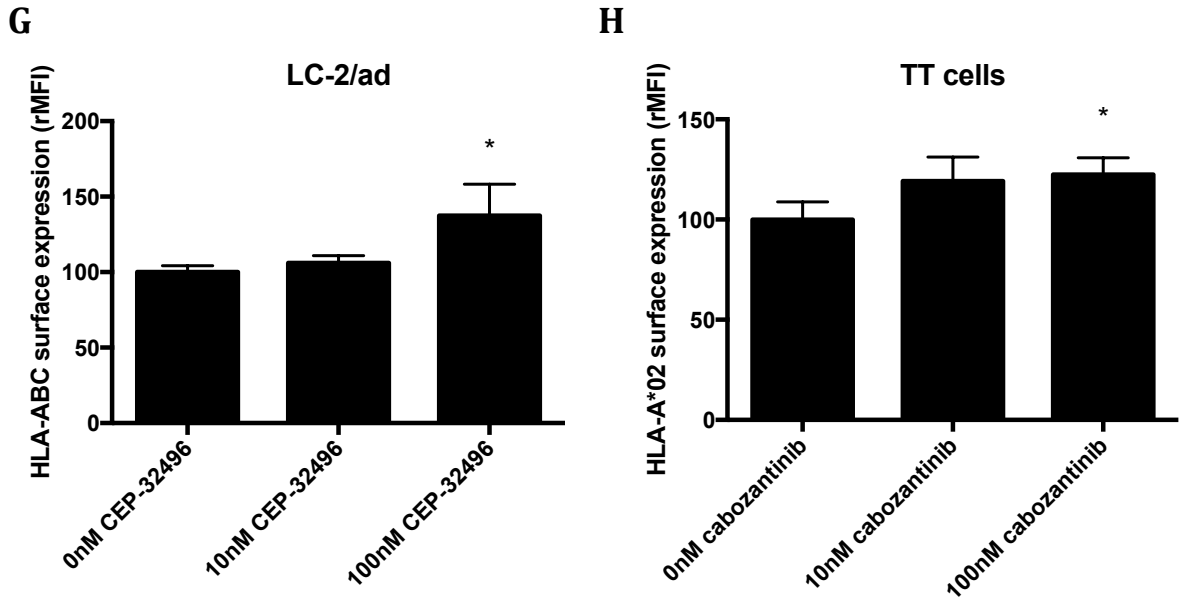
G**H**

Supplemental Figure S1: Increase in cell surface HLA depend on decrease in pERK in ALK inhibited ALCL cells.

Alectinib shuts down pERK expression in lysates of (A) Karpas 299 and (B) SUDHL-1 treated with inhibitor for 3 hrs. Alectinib upregulates cell surface HLA in (C) Karpas 299 and (D) SUDHL-1 cells at 72hrs. (E) Time course of HLA levels in Karpas cells treated with ALK inhibitors at day 0. At 4 and 6 days, cells show upregulation of HLA. After that time course was stopped because control cells were too dense. (F) Representative flow histograms for ALK inhibition. (G) Crizotinib does not decrease pERK levels in a EML4-ALK cell line H2228, hence (H) no increase in surface HLA is seen. Ceritinib decreases pERK levels very slightly and have a corresponding slight increase in HLA. At higher doses of drug tested, the cells did not survive. All flow cytometry was performed in triplicate. HLA-A,B,C was measured by the W6/32 antibody.

Supplemental Figure S2

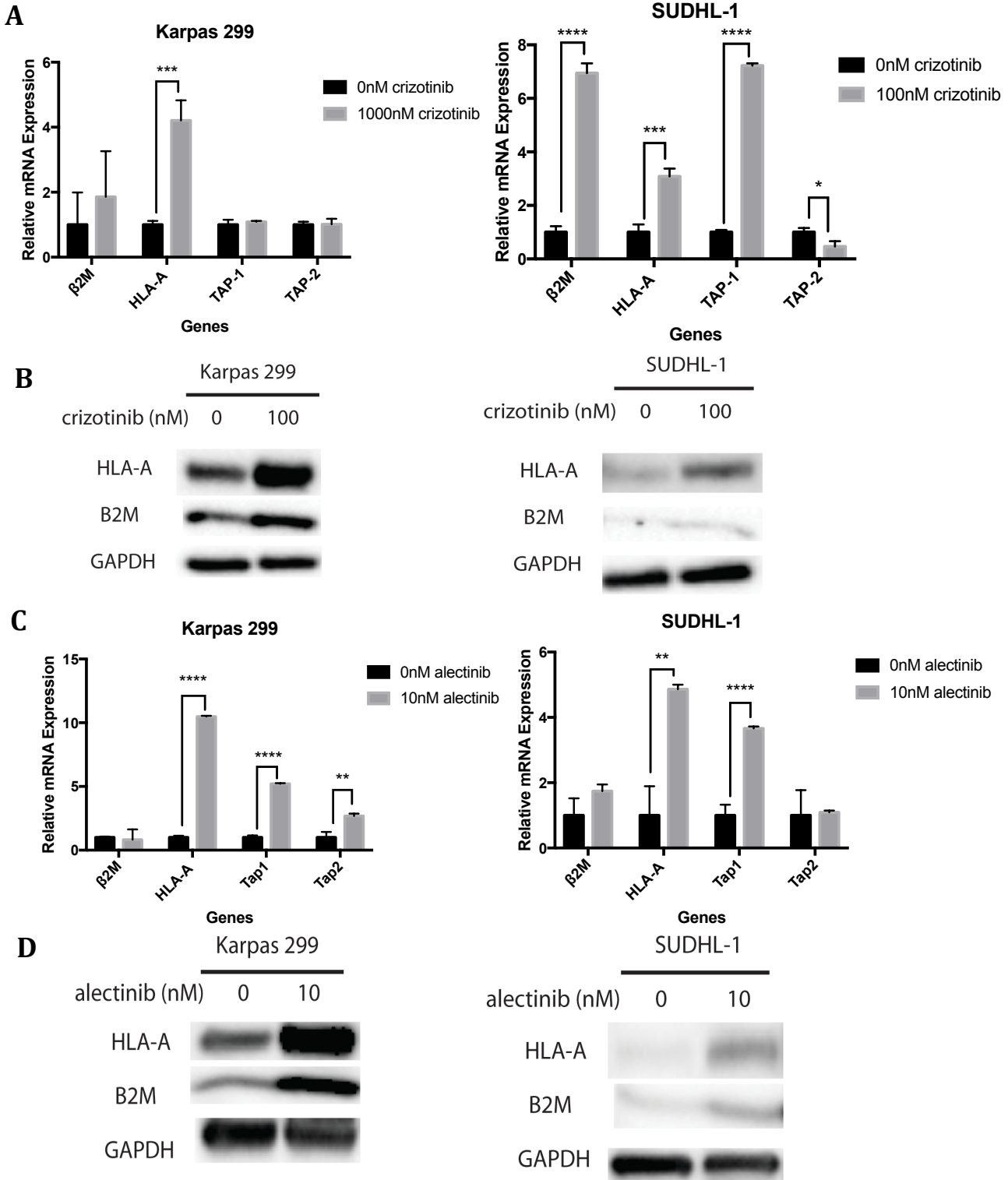




Supplemental Figure S2: RET inhibition leads to increase HLA.

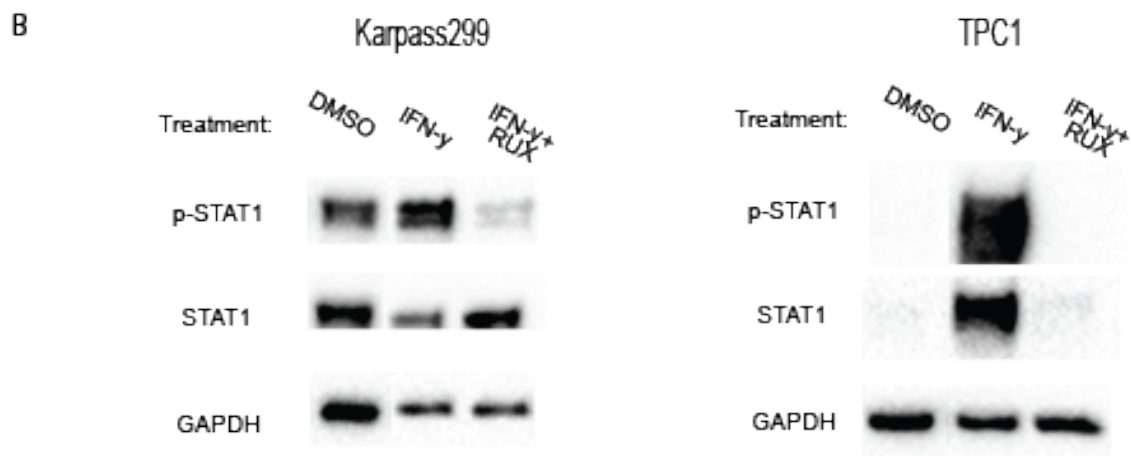
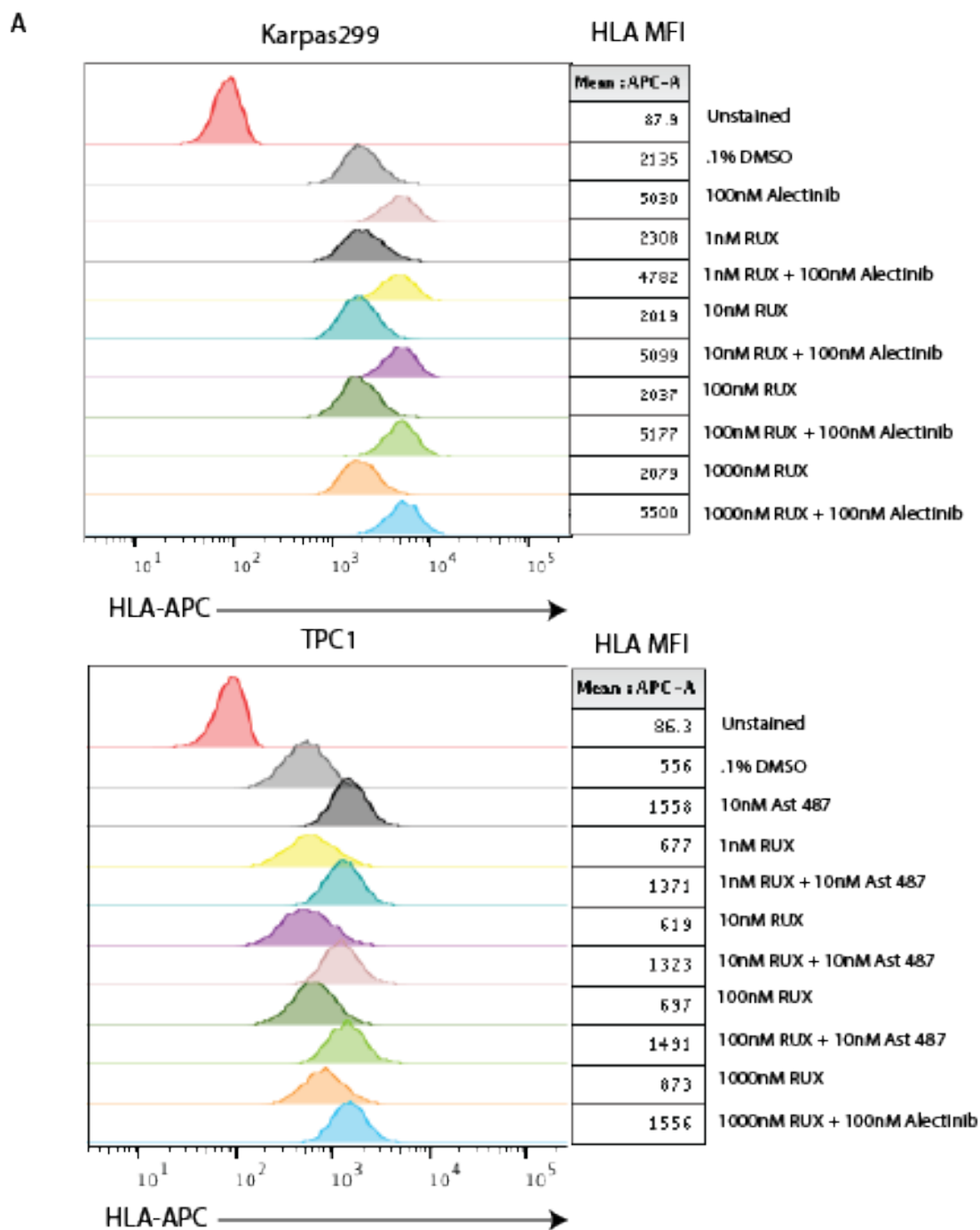
Surface HLA-A,B,C after 72hrs of RET inhibition in TPC1 cells, using (A) AST487, (B) BLU6864, and (C) cabozantinib. (D) TPC1 surface HLA-A*02 and HLA-A,B,C after treatment with RET siRNAs after 96hrs. HLA is measured after AST487 treatment for 72hrs in two other RET mutant cell lines (changes are significant $p < 0.05 - 0.001$), (E) TT cells (a medullary thyroid carcinoma cell line with a mutation of RET leading to a cysteine to tryptophan substitution) and (F) LC-2/ad (a lung adenocarcinoma harboring the CCDC6-RET fusion). Small changes in cell surface HLA with treatment of two other RET inhibitors, (G) CEP-32496 and (H) cabozantinib. All flow cytometry was performed in triplicate. HLA-A,B,C was measured by the W6/32 antibody. HLA-A*02 was measured by the BB7 antibody.

Supplemental Figure S3



Supplemental Figure S3: Increase in antigen processing machinery transcript and protein in ALK inhibited ALCL cells.

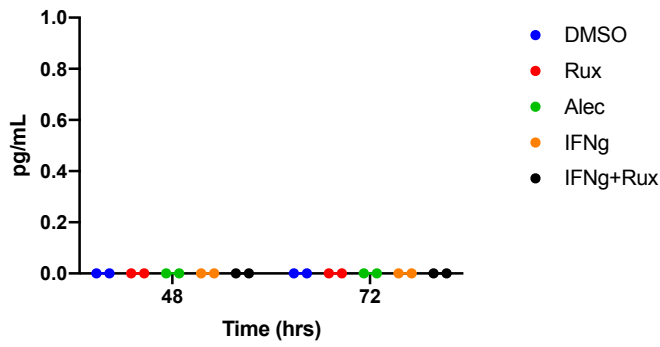
(A) qPCR of ALCL lines treated with crizotinib for 48hrs show increase in HLA and antigen processing machinery transcript levels. (B) Western blots at 72hrs show increase in HLA and beta-2microglobulin protein. Alectinib treatment on two ALCL lines show similar increases in (C) transcript levels and (D) protein levels. qPCR assays were performed in technical triplicate.



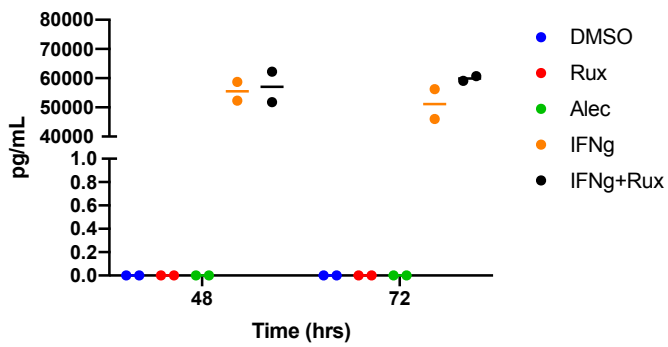
Supplemental Figure S4. (A) Karpas299 and TPC1 cells were treated with DMSO, Alectinib (100nM) or AST 487 (10nM), respectively, alongside various concentrations of ruxolitinib (RUX) for 72 hours, as indicated in the inset legend. Cells were harvested and stained with anti-HLA-A02 antibody (BB7-FITC) for flow cytometry. The top panel shows Karpas299 cells. Alectinib treatment leads to upregulation of HLA, which is unaffected by any concentration of RUX. The bottom panel shows TPC1 cells. AST 487 leads to upregulation of HLA, which is unaffected by any concentration of RUX. (B) Karpas299 and TPC1 cells were treated with DMSO, IFN- γ , or IFN- γ and RUX for 72 hours. Phosphorylated STAT1 (pSTAT1) is upregulated in both cell lines in response to IFN- γ treatment. Ruxolitinib inhibits pSTAT1 induction in both cell lines, confirming inhibitory action on JAK signaling.

Karpas299

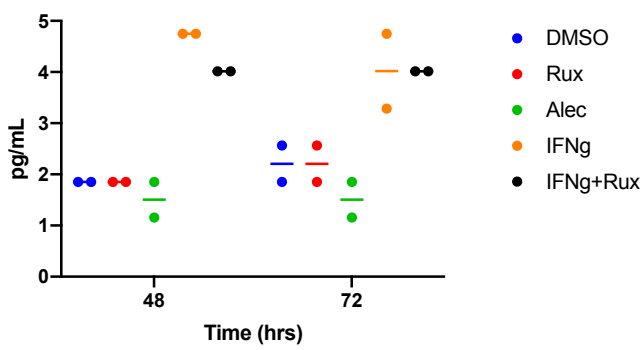
IFN α



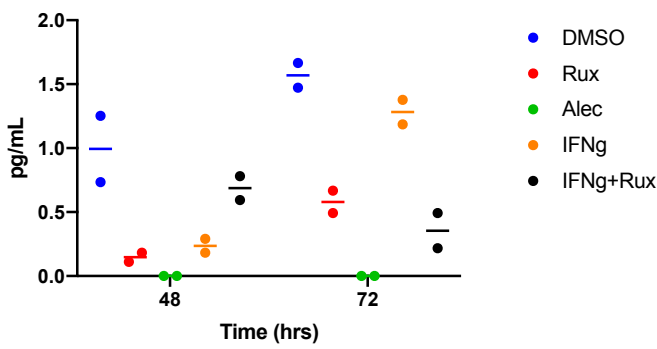
IFN γ



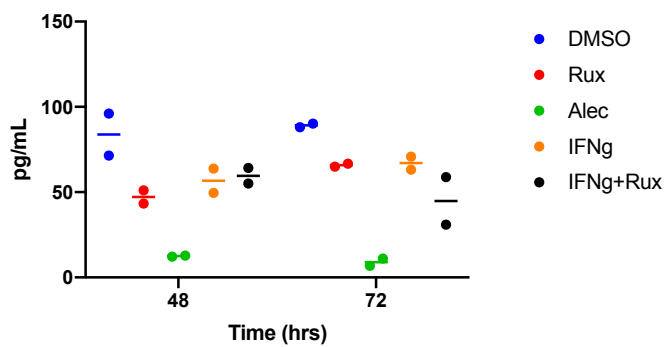
IL-4



IL-6

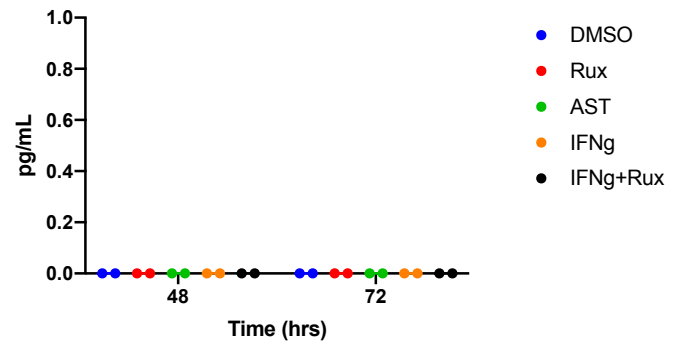


TNF α

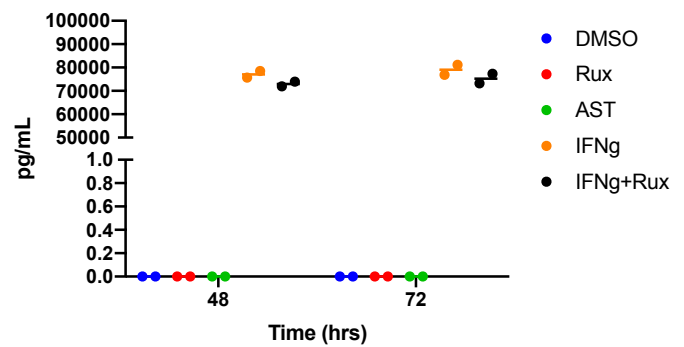


TPC1

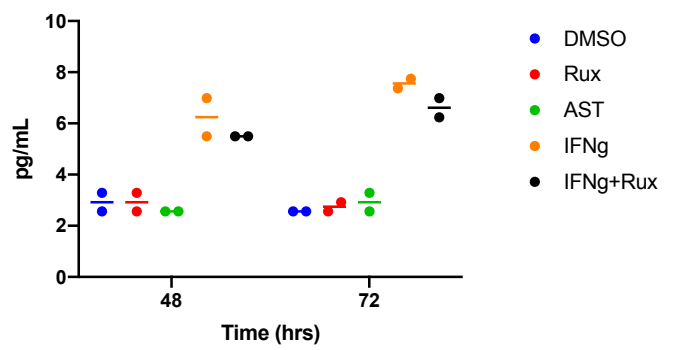
IFN α



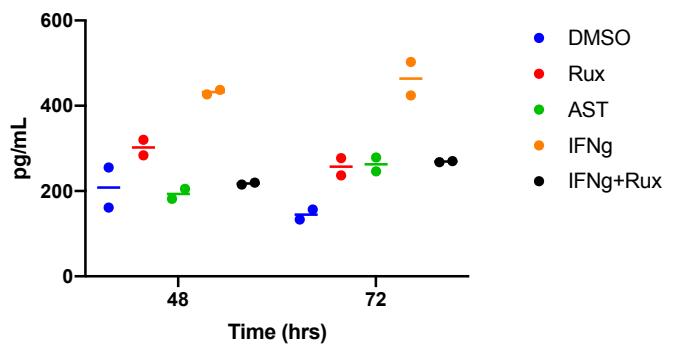
IFN γ



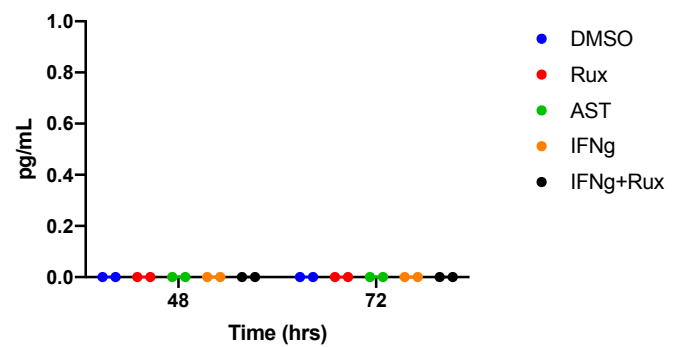
IL-4



IL-6

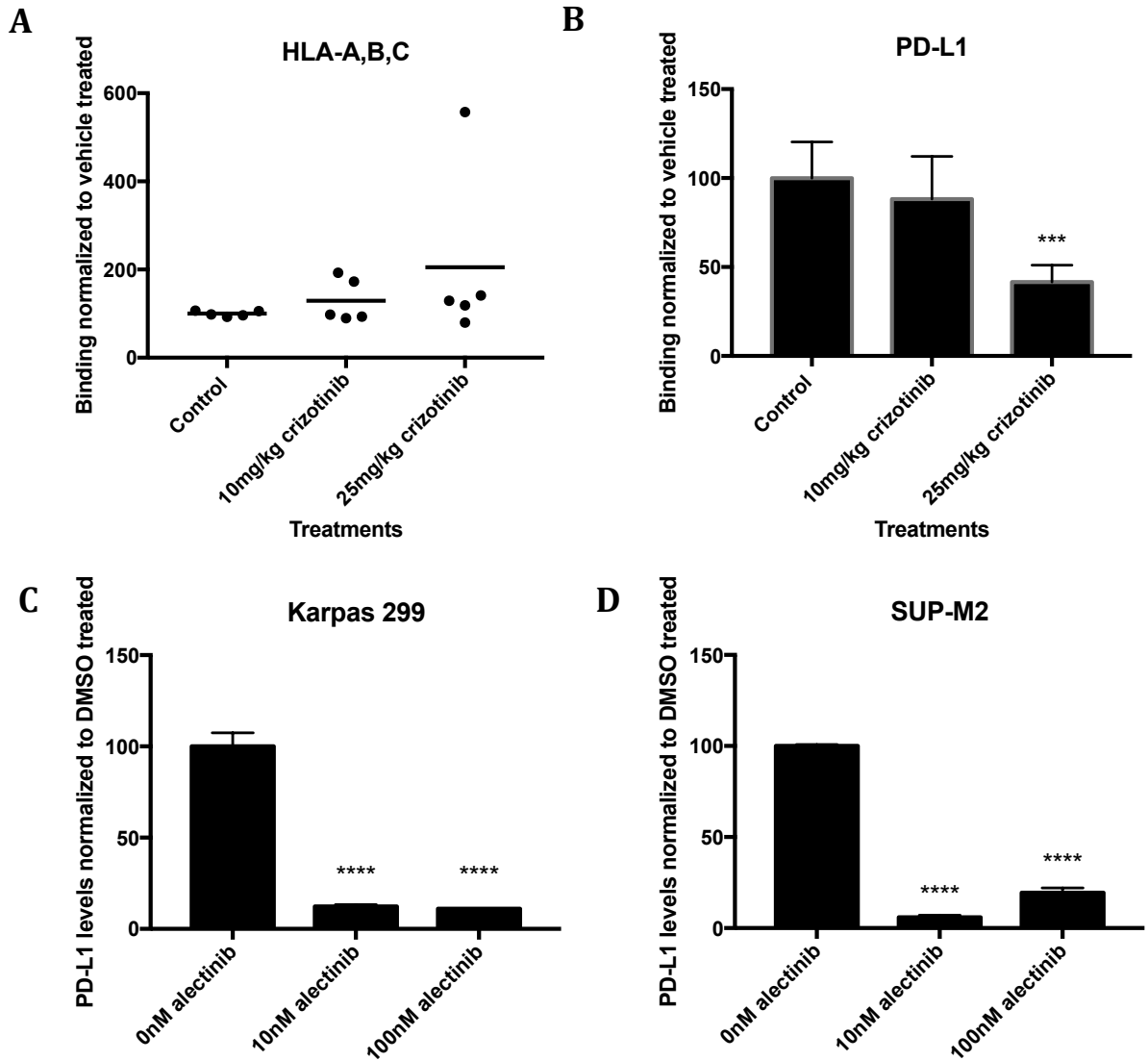


TNF α



Supplemental Figure S5: Karpas299 and TPC1 cells were treated with DMSO vehicle, 100nm alectinib (Alec) or 10nm AST487 (AST), respectively, for 48 and 72 hrs, as indicated by the inset legend. Supernatant media was harvested after treatment and analyzed by the Luminex device (Luminex Corporation, Austin, Texas) for relevant cytokine secretion. The left column shows data from Karpas299 and the right column is from TPC1 cells. On the left side of each panel is data after 24 hours. On the right side of each panel is data after 48 hours. Cytokines measured are noted on the top of each panel and displayed on the y axis in pg/ml. Alectinib inhibition in Karpas299 lymphoma had no effect on IFN α , IFN γ , IL4, and reduced IL6 and TNF α secretion. AST487 inhibition in TPC1 thyroid cells had no effect on IFN α , IFN γ , IL4, IL6 and TNF α secretion. Therefore, the ALK and RET inhibitors do not appear to act to upregulate the JAK/STAT pathway indirectly by increased cytokine release. As a positive control, IFN γ increased both IL4 and IL6 in these cells, which was reduced by 1000 nm ruxilutinib (Rux). IFN γ detected in the Luminex assay (50-70 ng/ml) is from the added IFN γ at 100ng/ml at time zero. Therefore, the increase in HLA after inhibitor treatment in these cell lines is not due to indirect activation of the JAK/STAT pathway via autocrine cytokine signaling.

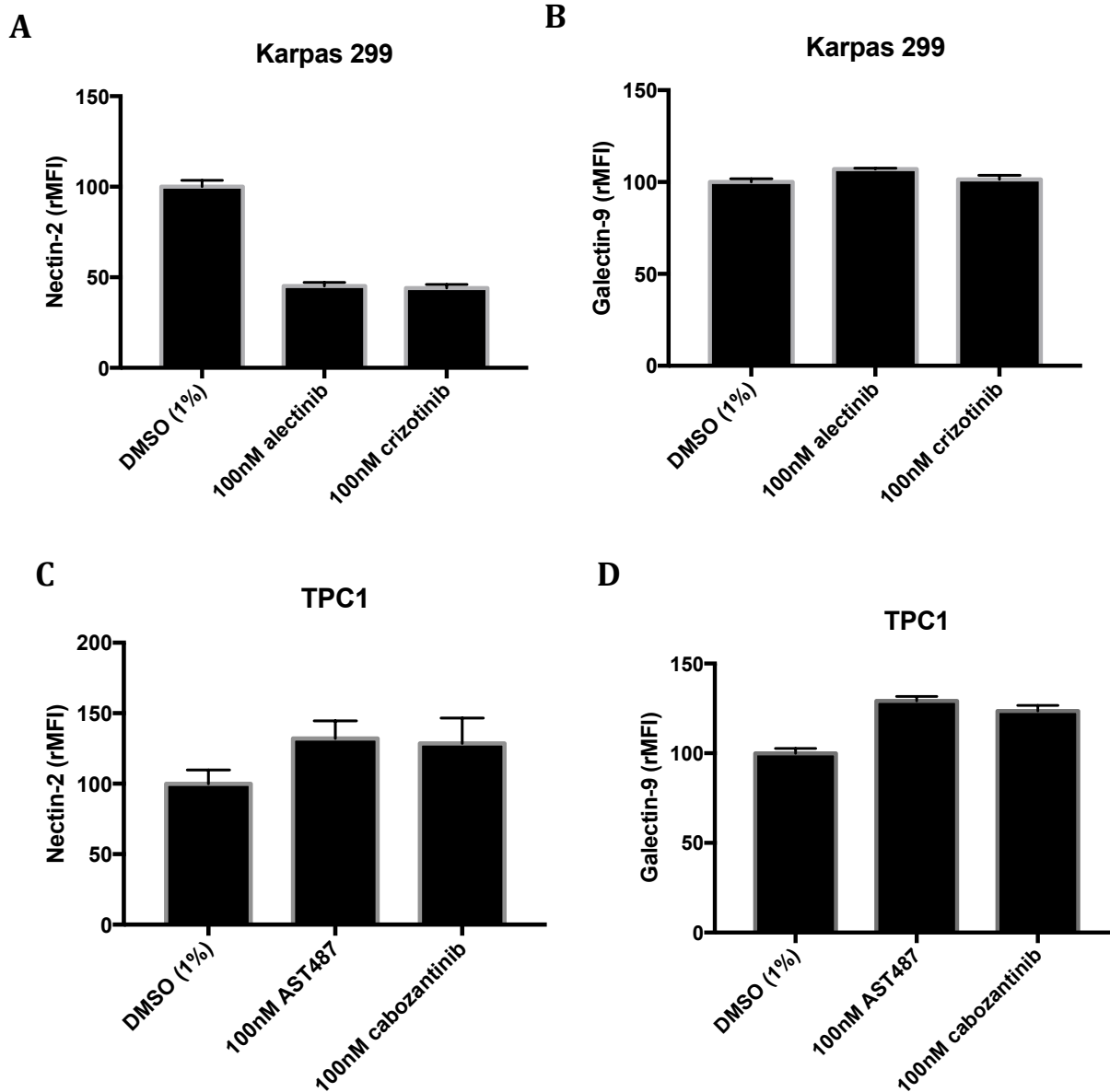
Supplemental Figure S6



Supplemental Figure S6: ALK inhibition in vivo and PD-L1 levels in vitro.

(A) Cell surface HLA-A,B,C expression of tumors isolated from NRG mice (n=5) subcutaneously injected with Karpas 299 and treated with crizotinib for 7 days through oral gavage. (B) PD-L1 levels decrease in vivo with crizotinib treatment of Karpas 299. PD-L1 levels after alectinib treatment in vitro in (C) Karpas 299 and (D) SUP-M2 (performed in triplicate).

Supplemental Figure S7

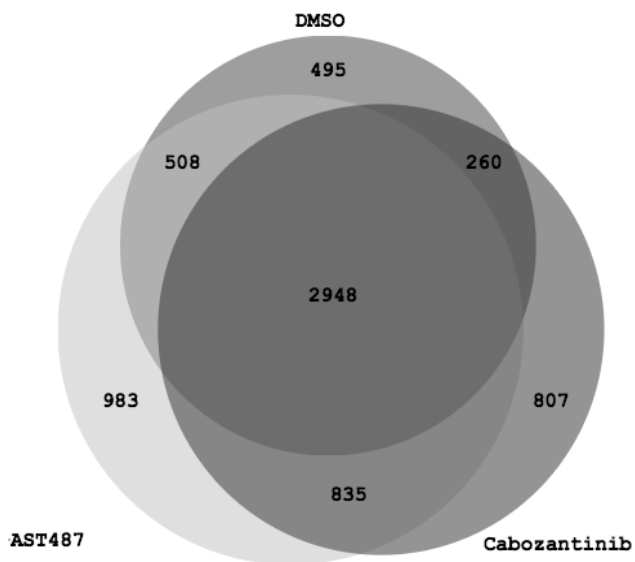


Supplemental Figure S7: Checkpoint ligands levels in response to ALK and RET inhibition.

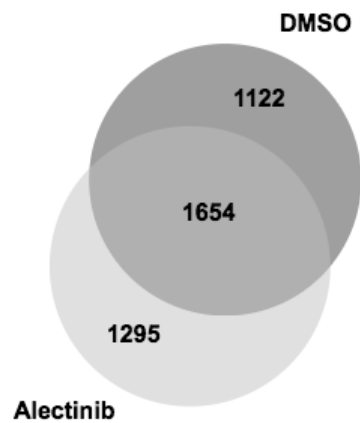
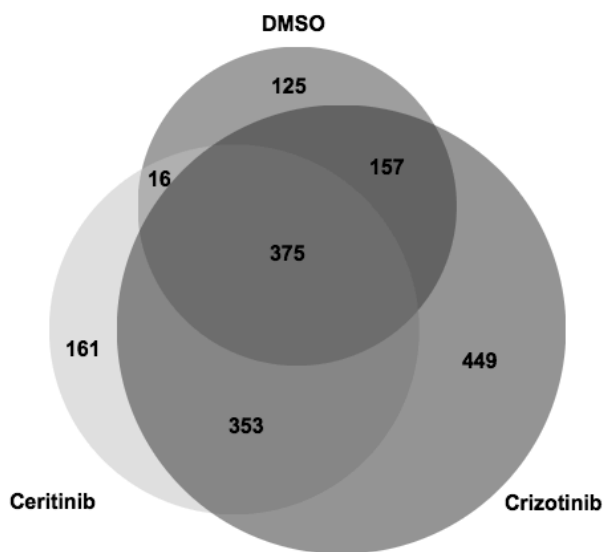
(A,B) Surface levels of nectin-2 and galectin-9 were measured after ALK inhibition by alectinib and crizotinib in Karpas 299 cells. (A,B) Surface levels of nectin-2 and galectin-9 were measured after RET inhibition by AST487 and cabozantinib.

Supplemental Figure S8

A



B

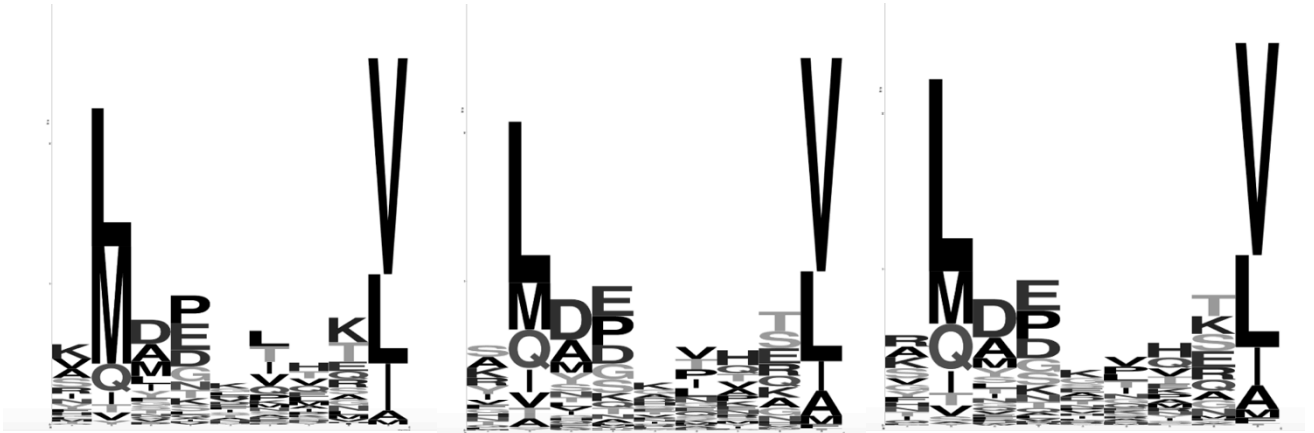


C

DMSO

AST487

Cabozantinib



D

Genes upregulated with AST487	
Gene Symbol	Fold Increase over DMSO
ATP6V0C	5.74
CPNE7	3.72
TMEM249	3.48
SCAND1	3.31
PLEC	3.16
TPM1	2.93
FLG	2.93
COL12A1	2.77
ALPK2	2.67
SCRIB	2.61
RASSF1	2.58
NCOR2	2.47
KRT80	2.47
FZD2	2.44
CLCN7	2.36
GAA	2.32
COL6A2	2.28
SLC7A5	2.25
SLC2A6	2.22
ZNF205	2.21
ASTN2	2.17
TIMM13	2.15
CLUH	2.11
FSCN1	2.09
EPHB1	2.09
TBL3	2.09
MYH9	2.08
PTK2B	2.07
AJUBA	2.02
SHARPIN	2.02
MGRN1	2.01
PLXNB2	2.00

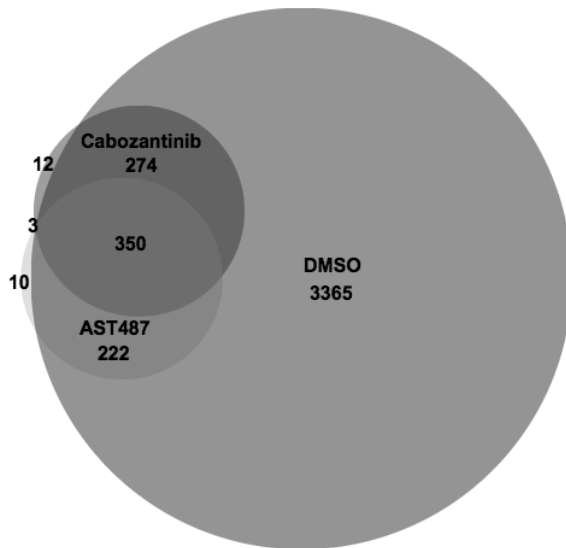
E

Genes upregulated with Cabozantinib	
Gene Symbol	Fold Increase over DMSO
COL12A1	5.80
TPM1	5.55
FLG	4.96
CPNE7	4.70
ASTN2	4.65
ALPK2	4.52
PTK2B	3.73
EPHB1	3.62
ZMYM6	3.29
SLC7A5	3.18
ATP6V0C	3.07
TLR5	3.04
AJUBA	3.02
HM13	2.93
PLEC	2.82
GAA	2.70
FZD2	2.63
ADAMTS3	2.61
SOX4	2.58
MYH9	2.51
ABCC4	2.50
CLCN7	2.48
ZNF33B	2.40
FLNB	2.40
UAP1L1	2.39
ZBTB12	2.38
SLC3A2	2.37
KRT80	2.37
TIPARP	2.35
ZNF71	2.34
AHR	2.33
APOL2	2.32
EPAS1	2.29
CPQ	2.29
HKDC1	2.26
JUP	2.26
SCAND1	2.22
TNS3	2.19
NCOR2	2.16

PPAN	2.15
PICK1	2.14
DPP4	2.14
PARP3	2.13
SLC2A6	2.10
MGRN1	2.09
TGFB111	2.08
VCAN	2.06
FCGRT	2.04
TBC1D2	2.00
PLIN2	2.00

F

AST487	Cabozantinib
FZD2	PLEC
COL6A2	SOX4
ZNF205	KRT80
MGRN1	JUP
	TBC1D2

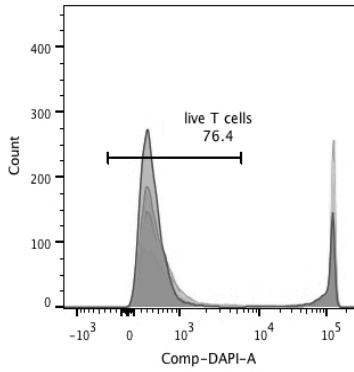
G

Supplemental Figure S8: Analysis of peptide repertoire changes after RET inhibition.

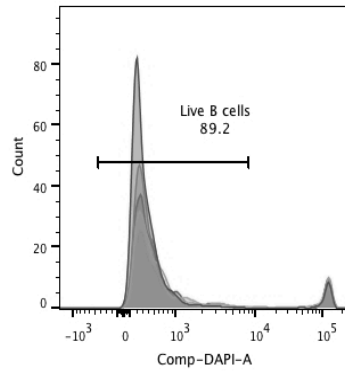
(A) Profile of eluted peptides found at least once in TPC1 cells treated with DMSO (control), 10nM AST487, or 100nM cabozantinib (n=3). (B) Profile of eluted peptides in Karpas 299 cells treated with DMSO, 100nM crizotinib, or 100nM ceritinib. (C) Comparison of motifs of all A*02 9-mer peptides eluted from mass spectrometry after control or RET inhibitor treatments. RNA-Seq data shows genes upregulated at least two-fold compared to control with (D) AST487 and (E) cabozantinib treatment. (F) Table of genes that had at least a two-fold increase in gene expression and whose peptides were detected in mass spectrometry. (G) Peptides found in at least 1 run in the control group compared to peptides found in all 3 runs in the RET inhibitor groups.

Supplemental Figure S9

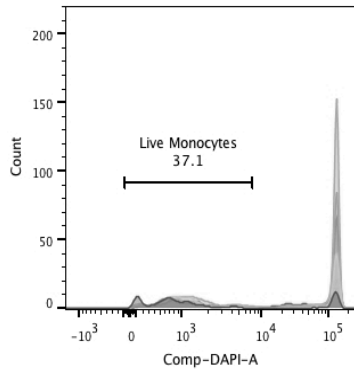
A



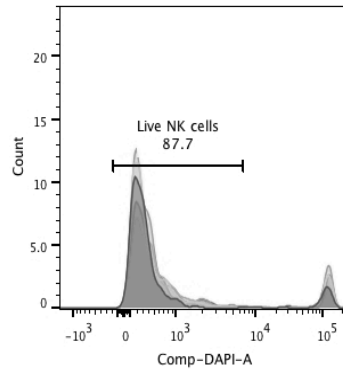
Sample Name	Subset Name
CD Markers_100nM Cabo_013.fcs	T cells
CD Markers_100nM Alectinib_011.fcs	T cells
CD Markers_10nM Alectinib_010.fcs	T cells
CD Markers_10nM AST487_012.fcs	T cells
CD Markers_DMSO_009.fcs	T cells



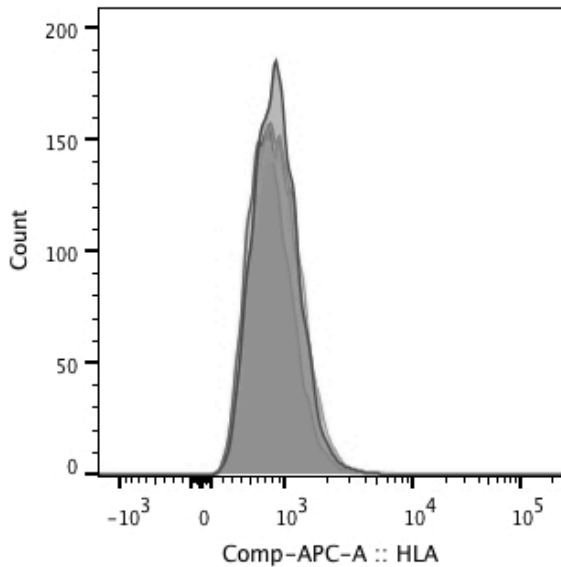
Sample Name	Subset Name
CD Markers_100nM Cabo_013.fcs	B cells
CD Markers_100nM Alectinib_011.fcs	B cells
CD Markers_10nM Alectinib_010.fcs	B cells
CD Markers_10nM AST487_012.fcs	B cells
CD Markers_DMSO_009.fcs	B cells



Sample Name	Subset Name
CD Markers_100nM Cabo_013.fcs	Monocytes
CD Markers_100nM Alectinib_011.fcs	Monocytes
CD Markers_10nM Alectinib_010.fcs	Monocytes
CD Markers_10nM AST487_012.fcs	Monocytes
CD Markers_DMSO_009.fcs	Monocytes



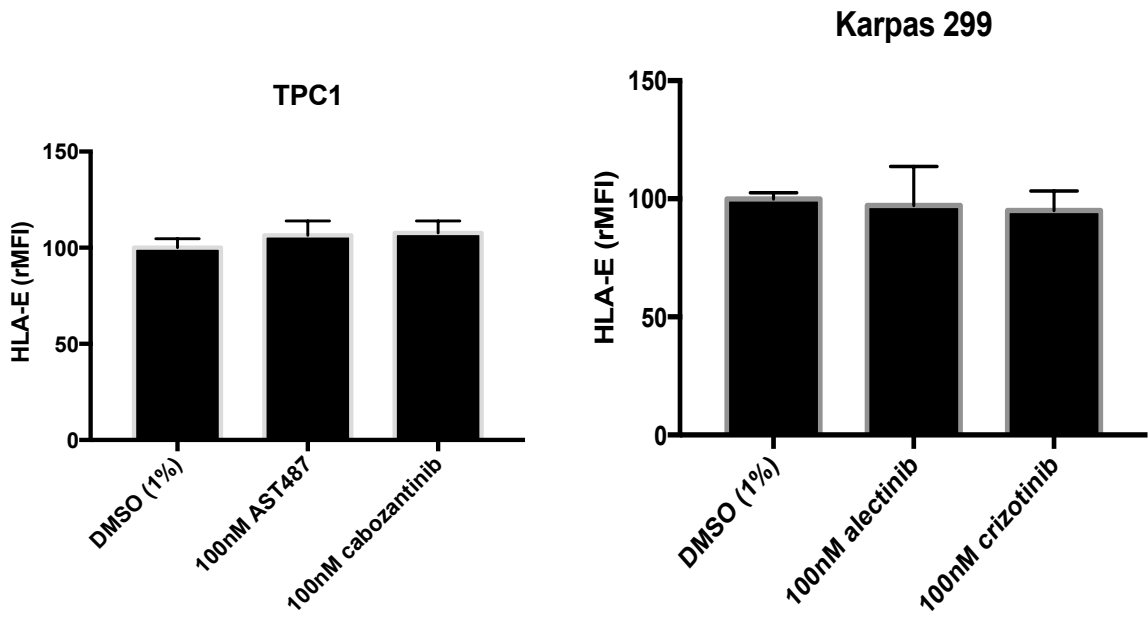
Sample Name	Subset Name
CD Markers_100nM Cabo_013.fcs	NK cells
CD Markers_100nM Alectinib_011.fcs	NK cells
CD Markers_10nM Alectinib_010.fcs	NK cells
CD Markers_10nM AST487_012.fcs	NK cells
CD Markers_DMSO_009.fcs	NK cells

B

	Sample Name	Subset Name
■	HLA+CD3_100nM Cabo_019.fcs	Live
■	HLA+CD3_100nM Alectinib_017.fcs	Live
■	HLA+CD3_10nM Alectinib_016.fcs	Live
■	HLA+CD3_10nM AST487_018.fcs	Live
■	HLA+CD3_DMSO_015.fcs	Live

Supplemental Figure S9: PBMC viability and HLA levels are not affected by inhibitors. (A) PBMCs were isolated and viability was measured with PI staining after incubation with ALK inhibitors, RET inhibitors, or control (DMSO). Different cell populations were gated and viability is displayed. (B) Flow histogram showing inhibitors do not affect HLA levels of isolated T cells.

Supplemental Figure S10



Supplemental Figure S10: HLA-E levels do not change with drug treatment. TPC1 cells were treated with AST487 and cabozantinib and surface HLA-E levels were measured after 72hrs. Similarly, Karpas 299 cells were treated with alectinib and crizotinib and HLA-E levels were measured.

Supplemental Table 1

Drug	HLA levels	Beta-2-microglobulin	TAP1	TAP2	PD-L1	Nectin	Galectin
AST487	↑	unchanged	↑	↑	unchanged	unchanged	unchanged
BLU6864	↑	↑	↑	unchanged	N/A	N/A	N/A
Cabozantinib	↑	↑	↑	unchanged	N/A	unchanged	unchanged
Alectinib	↑	unchanged	variable	variable	↓	↓	↓
Ceritinib	↑	↑	↑	variable	N/A	N/A	N/A
Crizotinib	↑	↑	variable	variable	↓	↓	↓

Supplemental Table 1: Summary of the inhibitors effects on HLA, antigen processing machinery, and checkpoint ligands